Performance assessment of a four-air cathode membraneless microbial fuel cell stack for wastewater treatment and energy extraction

Asimina Tremouli[1,*], *Pavlos K.* Pandis[1,2], *Theofilos* Kamperidis[1], *Vassilis N.* Stathopoulos[2], *Christos* Argirusis[1], and *Gerasimos* Lyberatos[1,3]

[1]School of Chemical Engineering, National Technical University of Athens, Heroon Polytechniou 9, 15780, Zografou Athens, Greece
[2]General Department, School of Sciences, National and Kapodistrian University of Athens, 34400 Psachna Campus, Evia, Greece
[3]Institute of Chemical Engineering Sciences (ICE-HT), Stadiou Str., Platani, 26504, Patras, Greece

Abstract. A stack of two identical single chamber microbial fuel cells (MFCs) was assessed during using fermentable house hold extract as substrate. The design of the MFC units was based on the single chamber membrane-less technology using four cathode electrodes. The total power output was 492 mW either in series or parallel connection considering a total anolyte volume of 240 cm^3. During continuous operation, the COD removal was 80% for each cell and for both operation modes (series and parallel). The electrochemical profiles provided significant information on the behaviour of the stack. During continuous operation, parallel connection is preferred over series connection, as it results to the same power output values, and COD removal but it provides lower internal resistances leading to more stable electrochemical performance behaviour.

1 Introduction

Microbial fuel cells (MFCs) are bio-electrochemical devices which convert biomass spontaneously into electricity via the contribution of microorganisms [1, 2]. The advantage of MFCs to generate electricity while treating wastewater has attracted scientists' attention as this benefit makes the technology a promising alternative to the use of energy consuming treatment processes in wastewater treatment plants (i.e. aerated activated sludge process). The main challenge in the effort to render MFC technology practically implementable is to increase the relatively low power output, while keeping the cost low [3]. In this direction, several designs and different materials have been suggested [4, 5] Scale-up has been proposed either by increasing the size of the MFC [6] or by multiplying and stacking relatively small multiple MFC units [7]. In any case, an MFC remains a complex system that involves a number of technological, electrochemical and microbiological aspects, which need to be understood before the technology can be implemented in practice and in real life environments. Electrochemical Impedance Spectroscopy (EIS) is a technique

---

* Corresponding author: atremouli@chemeng.ntua.gr

widely used to give an insight to the electrochemical phenomena in fuel cells [8–11]. This technique has become a valuable and in-depth understanding tool for phenomena occurring in individual MFC units as well as in MFC stacks [12, 13].

This study reports on the performance of a stack comprised of two identical MFC units. The stack has been constructed aiming at keeping the cost low. Thus GORE-TEX cloth was used as separator and cathode catalyst support, while MnO_2 was used as catalyst [14, 15]. The units were operated in continuous mode under two different connection modes (series and parallel) using fermentable household food waste (FORBI) extract as the feed [16]. The stack connection modes were evaluated through Linear Sweep Voltammetry (LSV) by assessment of the maximum power output and through Electrochemical Impedance Spectroscopy measurements (EIS) for the interpretation of the electrochemical processes, which occur under continuous operation.

2 Materials and methods

2.1 MFC set-up and operation

The experiments were conducted using a stack comprising of two identical, membrane-less single chamber, four air-cathode MFCs. Each cell (cell 1 and cell 2) consists of a single cubical compartment and four plexiglas tubes run through it. The working volume of each unit is 120 ml. The manufacturing process is presented in detail in [17]. Each cell was filled with graphite granules (Ø1.5–5 mm, type 00514, Le Carbone, Belgium), serving as the anodic biofilm support and conducting material (conveying electrons to the graphite rod placed through the packed bed of granules) [17]. In order to remove the metals from the surface and the inner pores of the granules, the granules were washed for 24 h in 32% HCL, the process being repeated four times [18]. The cathode tubes are open to the atmosphere and no special aeration is employed. GORE-TEX ® cloth is used as a separator and as a catalyst (MnO_2) support of the cathode electrocatalyst, which was MnO_2 [14]. The catalytic paste activation of the cloth both as a catalyst and an electrical conductor was prepared according to the methods proposed by [19]. The two MFCs were operated in a permanently air-conditioned room at 20°C, in order to minimize the temperature fluctuations.

Prior to the continuous operation, the MFCs were operated and acclimated in batch mode as described in detail elsewhere [12, 17]. The enrichment and adaptation of the electrochemically active bacteria were performed during the first batch cycles. The inoculum was anaerobic sludge obtained from the Athens (Greece) Wastewater Treatment Plant. During the acclimation period the feedstock consisted of 10 % v/v anaerobic sludge, 0.8 g COD L^{-1} glucose (used as electron donor), a buffer solution and some trace elements. Following the inoculation period glucose was replaced by FORBI extract, without further addition of sludge and trace elements. FORBI was produced by drying and shredding the pre-sorted fermentable fraction of household food waste collected door-to-door in the Municipality of Halandri, Athens, Greece [16, 17, 20]. The electrode output for each MFC was individually recorded, at 1min intervals, in volts (V) versus time using a data acquisition system (Advantech ADAM-4019+) [17]. The load of the feed was 1.6 g COD L^{-1}. Thence, the operation of the MFCs was switched to continuous feeding. The feed characteristics were not varied (1.6 g COD L^{-1}). The continuous feeding was achieved by the use of a peristaltic pump (Masterflex, Cole-Parmer Instrument Company). The flow rate was adjusted at 0.13 ml/min, corresponding to 15 h hydraulic retention time, HRT.

2.2 Electrochemical characterization

Electrochemical measurements were conducted using a Potentionstat – Galvanostat (BIOLOGIC SP-150) equipped with a frequency response analyzer (FRA). Linear Sweep Voltammetry (LSV) was performed from Open Circuit Voltage (OCV) to short circuit with 1 mV/s step. Power output was expressed in mW considering a total anodic liquid volume of 240 cm^3. Electrochemical Impedance Spectroscopy (EIS) measurements were conducted to export bode-bode (Nyquist) plots at OCV and short circuit over the frequency range of 100 kHz –1 mHz, using a stimulus of 10 mV amplitude. All the above were conducted at the stack of the cells (both at parallel and series connections) using a three electrode setup (Working Electrode (WE), Counter Electrode (CE) and Saturated Calomel Electrode-SCE as the reference electrode (RE)) after OCV was reached in each cell applying no external resistance. The values of internal resistances of the cell were calculated through EC-Lab software Z-fit analysis considering a two time constant model equivalent circuit. The experimental fitting was applied considering the solution resistance of the cell (R_S) in series with two parallel R_Q components. R_{CT} is defined as the charge transfer resistance, R_{BF} the biofilm resistance, Q_{CT} and Q_{BF} the capacitance of charge transfer and biofilm respectively and Warburg element (W) as the diffusion impedance as reported elsewhere [12, 17, 21].
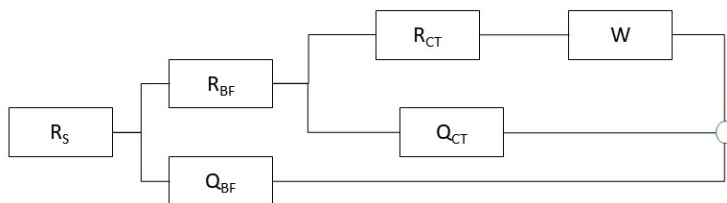

Fig. 1. Equivalent circuit used for EIS Z-Fit analysis.

3 Results and discussion

3.1 Continuous operation of the cells

Following inoculation, the system performance was examined in continuous mode using FORBI as substrate (FORBI, 1.6 g COD L^{-1}). The variations of the cells' voltage during continuous flow are presented in Figure 2. The MFCs exhibited good stability over an operational period of 110 h. During this period, the steady-state cell voltage was equal to 442 ± 0.02 mV for the cell 1 and equal to 380 ± 0.02 mV for the cell 2. Moreover, the COD removal was equal to 80% for both cells while the pH and the conductivity remained approximately constant during continuous operation (cell 1: pH 7.57 ± 0.1, 9.43 ± 0.08 mS·cm^{-1} and cell 2: pH 7.36 ± 0.23, 8.79 ± 0.52 mS·cm^{-1}). After 40.1 h of continuous operation, the system was considered already at steady state and EIS experiments were conducted. From Figure 3, the LSV curves depict the maximum power output from the two connection modes of the cells (parallel and series). Both modes resulted in a total power output of 4.92 mW per total anolyte volume. The curent continuos opertation resulted in larger output values in comparison with batch operation of the same cathodic and anodic electrodes [17] totally atributed to continuous regeneration of the FORBI substrate [3, 13]. The COD removal percentage was found in same values in comparison with batch operation [17], which indicates the efficient capacity of the stack during contunuous operation.
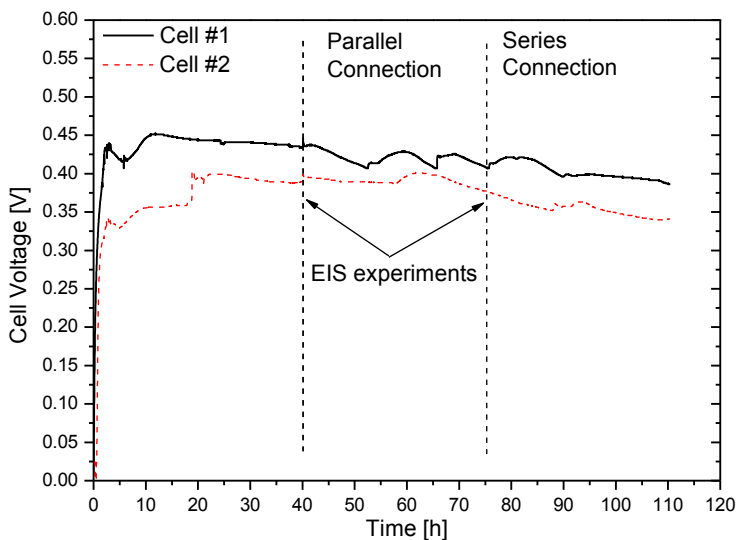
Fig. 2. Voltage of each cell versus time during continuous operation. Cell 1 and Cell 2 with FORBI substrate (FORBI 1.6 g COD L^{-1}, at the inlet). The arrows indicate the time when EIS experiments occurred during operation.
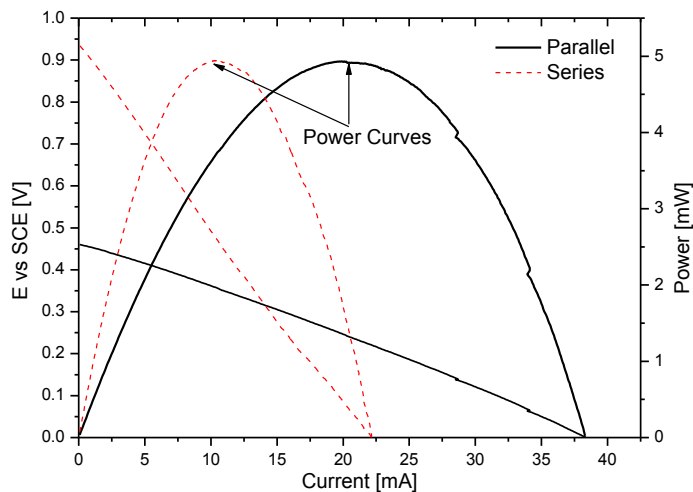

Fig. 3. Linear Sweep Voltammetry (LSV) curves and maximum power output of the stack under continuous operation in parallel and series connection.

3.2 Electrochemical assessment of the stack

In Figure 4, Nyquist diagrams are presented for both operation modes of the stack during continuous operation.
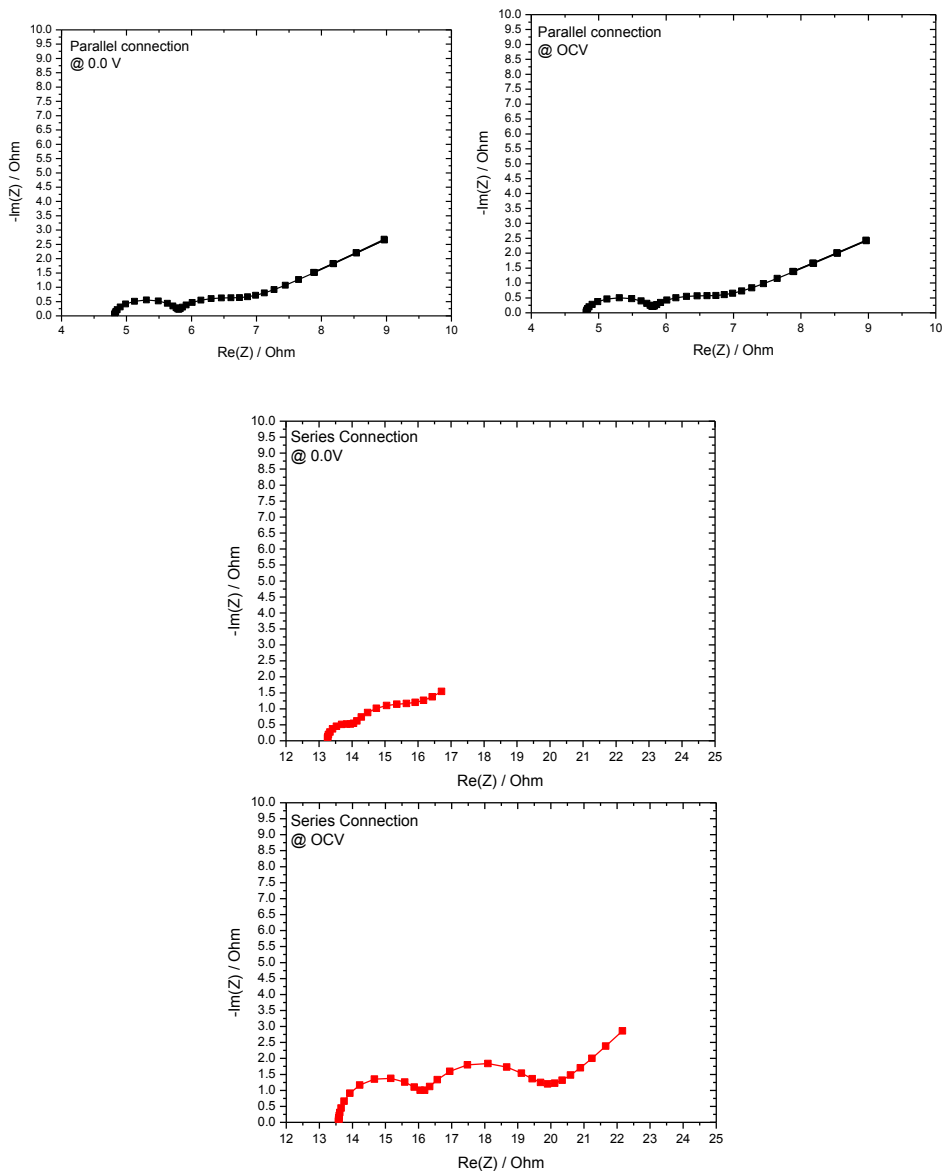
Fig. 4. EIS results (Nyquist diagrams) for parallel and series connection of the stack OCV and at short circuit. (Top row: parallel connection, bottom row: series connection).

The total internal resistance for the parallel mode is lower than for the series mode, indicating the occurrence of different electrochemical processes in the two configurations. The range of internal resistances of the cells are still lower in comparison with the internal resistances of a dual-chamber MFC [14]. Two arcs are observed in all diagrams, followed by a straight line with ~45° slope at the end (Warburg element). The first arc is associated with biofilm development which remains at a steady value of RBF ~1 Ω for both the parallel and series modes @OCV as reported in Table 1. The capacitance of the biofilm, on the other hand, is by far lower in the series connection case, which implies

a non-sustainable connection in series as far as maintaining a fast and gradual biofilm development. Thus, the $R_{BF} = 2.77 \, \Omega$ (value in series @ 0.0V) is found higher [21]. The second arc that describes the charge transfer resistance validates the results during biofilm development as charge transfer is totally related to biofilm behaviour. According to Sekar et al [22], this phenomenon is observed during biofilm formation, and is followed by an increase in the anodic reaction rates (R_{CT}). It is totally attributed to direct electron transfer by microbial consortia during the operation. Finally, the comparison between parallel and series connection configurations, favors the former connection as lower internal resistances occur, for the same COD removal percentage and maximum power output.

Table 1. Fitting results on EIS experiments on MFC stack under continuous operation.

Fitted Parameters	Parallel		Series	
	EIS at OCV	EIS at 0.0V	EIS at OCV	EIS at 0.0V
R_S (Ω)	8.81	8.95	13.25	13.58
R_{BF} (Ω)	1.00	0.91	1.00	2.77
Q_{BF} (F)	$2.7 \cdot 10^{-3}$	$3.1 \cdot 10^{-3}$	$17.5 \cdot 10^{-6}$	$0.1 \cdot 10^{-6}$
Q_{CT} (F)	0.24	0.29	$1 \cdot 10^{-3}$	$3 \cdot 10^{-3}$
R_{CT} (Ω)	0.84	0.91	1.49	3.1
R_{INT} (Ω)	10.65	10.77	15.74	19.45

4 Conclusions

The operation of the stack consisting of two single-chamber MFC units, during continuous operation provided lower internal resistances, higher power output values and the same COD removal percentage than their operation in batch modes [17]. This occurred during parallel and series connections using FORBI as substrate. The most preferable operation though seems to be the parallel mode since the electrochemical assessment demonstrated a superior overall stack performance for this configuration.

References

1. H. P. Bennetto, Biotechnology Education **1**, 163–168 (1990)
2. N. Lu, S. Zhou, J. T. Zhang, J. R. Ni, Biochem. Eng. J. **43**, 246–251 (2009)
3. B. E. Logan, *Microbial Fuel Cells* (John Wiley & Sons, New Jersey, 2008)
4. M. Behera, P. S. Jana, M. M. Ghangrekar, Bioresour. Technol. **101**, 1183–1189 (2010)
5. A. N. Ghadge, M. M. Ghangrekar, Appl. Microbiol. Biotechnol. **85**, 1665–1671 (2010)
6. H. Liu, S. Cheng, L. Huang, B. E. Logan, J. Power Sources **179**, 274–279 (2008)
7. I. Ieropoulos, J. Greenman, C. Melhuish, Int. J. Energy Res. **32**, 1228–1240 (2008)
8. H. Gasparyan, C. Argirusis, C. Szepanski, G. Sourkouni, V. Stathopoulos, T. Kharlamova, V. A. Sadykov, S. Bebelis, ECS Trans. **25**, 2681–2688 (2009)
9. H. Gasparyan, S. Neophytides, D. Niakolas, V. Stathopoulos, T. Kharlamova, V. Sadykov, O. Van der Biest, E. Jothinathan, E. Louradour, J. P. Joulin, S. Bebelis, Solid State Ion **192**, 158–162 (2011)

10. P. Pandis, T. Kharlamova, V. Sadykov, V. N. Stathopoulos, MATEC Web of Conferences **41**, 04001 (2016a)

11. P. K. Pandis, E. Xenogiannopoulou, P. M. Sakkas, G. Sourkouni, C. Argirusis, V. N. Stathopoulos, RCS Adv. **6**, 49429–49435 (2016)

12. A. Tremouli, P. K. Pandis, I. Karydogiannis, V. N. Stathopoulos, C. Argirusis, G. Lyberatos, Global Nest J. **Accepted** (2019)

13. D. Hidalgo, A. Sacco, S. Hernández, T. Tommasi, Bioresour. Technol. **195**, 139–146 (2015)

14. A. Tremouli, A. Intzes, P. Intzes, S. Bebelis, G. Lyberatos, J. Appl. Electrochem. **45**, 755–763 (2015)

15. A. Tremouli, M. Martinos, S. Bebelis, G. Lyberatos, J. App. Electrochem. **46**, 515–526 (2016)

16. D. Chatzikonstantinou, A. Tremouli, K. Papadopoulou, G. Kanellos, I. Lampropoulos, G. Lyberatos, Waste Manage. & Res. 1–6 (2018)

17. A. Tremouli, I. Karydogiannis, P. K. Pandis, K. Papadopoulou, C. Argirusis, V. N. Stathopoulos, G. Lyberatos, Energy Procedia, **Accepted** (2019)

18. S. Freguia, K. Rabaey, Z. Yuan, J. Keller, Electrochim. Acta **53**, 598–603 (2007)

19. L. Zhouang, S. Zhou, Y. Wang, C. Liu, S. Geng, Biosens. Bioelectron. **24**, 3652–3656 (2009)

20. I. Ntaikou, N. Menis, M. Alexandropoulou, G. Lyberatos, Bioresour. Technol. **263**, 75–83 (2018)

21. X. Dominguez-Benetton, S. Sevda, K. Vanbroekhoven, D. Pant, Chem. Soc. Rev. **41**, 7228–7246 (2012)

22. N. Sekar, R. P Ramasamy, J. Micr. & Biochem. Tech. **S6**, 004, (2013)